A simple and fast method for solving the time-dependent Bloch equations in spin-locked chemical exchange saturation transfer (CESTrho) magnetic resonance imaging

Kenya Murase[1], and Shigeyoshi Saito[1]

[1]*Department of Medical Physics and Engineering, Osaka University Graduate School of Medicine, Suita, Osaka, Japan*

INTRODUCTION

Recently, there has been an increasing number of studies that have used the chemical exchange effect to probe the tissue microenvironment and provide novel imaging contrasts that are not available from conventional magnetic resonance imaging (MRI) techniques. Most of these studies adopted either a chemical exchange saturation transfer (CEST) or a spin-locking (SL) approach [1]. Jin et al. [1] performed CEST and SL experiments to compare the characteristics of the CEST and SL approaches in the study of chemical exchange effects. Kogan et al. [2] developed a new method to measure proton exchange which combines CEST and SL methods (CESTrho). CESTrho contrast mechanism, however, is complex, depending not only on the concentration of CEST agents, exchange and relaxation properties, but also varying with experimental conditions such as magnetic field strength and radiofrequency (RF) power. Thus, for investigating these optimal conditions, numerical simulations are useful and effective. To perform extensive numerical simulations for CESTrho MRI, it will be necessary to develop a simple and fast method for obtaining the numerical solutions to the time-dependent Bloch equations. Then, the purpose of this study was to demonstrate a simple and fast method for solving the time-dependent Bloch equations in CESTrho MRI using the 2-pool CEST model [3].

MATERIALS AND METHODS

The Bloch equations in the 2-pool CEST model are given by $d\mathbf{M}(t)/dt=\mathbf{A}\cdot\mathbf{M}(t)$...(1) [3], where $\mathbf{M}(t)=[M_x^a(t)\ M_x^b(t)\ M_y^a(t)\ M_y^b(t)\ M_z^a(t)\ M_z^b(t)\ 1]^T$ and superscripts *a* and *b* show the parameters in pool a and pool b, respectively. For example, $M_x^a(t)$ denotes the x component of the magnetization in pool a at time *t*. **A** in Eq. (1) is given by Eq. (2), where R_1^a ($=1/T_1^a$) and R_2^a ($=1/T_2^a$) denote the longitudinal and transverse relaxation rates in pool a, respectively, R_1^b ($=1/T_1^b$) and R_2^b ($=1/T_2^b$) those in pool b, k_a the exchange rate from pool a to pool b, k_b the exchange rate from pool b to pool a, and M_0^a and M_0^b the thermal equilibrium z magnetizations in pool a and pool b, respectively. $\Delta\omega_a$ and $\Delta\omega_b$ are given by $\omega_a-\omega$ and $\omega_b-\omega$, respectively, where ω_a and ω_b are the Larmor frequencies in pool a and pool b, respectively, ω is the frequency of RF irradiation, and ω_1 is the nutation rate of the RF irradiation. The solution of Eq. (1) can be given by $\mathbf{M}(t)=e^{\mathbf{A}t}\cdot\mathbf{M}(0)$...(3) [3], where $\mathbf{M}(0)=[0\ 0\ 0\ 0\ M_0^a\ M_0^b\ 1]^T$ and $e^{\mathbf{A}t}$ is the matrix exponential that can be computed using diagonalization [3].

$$\mathbf{A}=\begin{pmatrix} -(R_2^a+k_a) & k_b & \Delta\omega_a & 0 & 0 & 0 & 0 \\ k_a & -(R_2^b+k_b) & 0 & \Delta\omega_b & 0 & 0 & 0 \\ -\Delta\omega_a & 0 & -(R_2^a+k_a) & k_b & \omega_1 & 0 & 0 \\ 0 & -\Delta\omega_b & k_a & -(R_2^b+k_b) & 0 & \omega_1 & 0 \\ 0 & 0 & -\omega_1 & 0 & -(R_1^a+k_a) & k_b & R_1^aM_0^a \\ 0 & 0 & 0 & -\omega_1 & k_a & -(R_1^b+k_b) & R_1^bM_0^b \\ 0 & 0 & 0 & 0 & 0 & 0 & 0 \end{pmatrix}\cdots(2)$$

Figure 1 illustrates the magnetization in the rotating frame in the case when spins are locked by an SL pulse that is applied on the x-axis at an offset frequency Ω. The effective SL field (B_1^{eff}) is given by $B_1^{eff}=(\omega_1^2+\Omega^2)^{1/2}/\gamma$, where γ is the gyromagnetic ratio. To achieve SL, the magnetization is first flipped by the θ-degree pulse to the x-z plane, then locked by B_1^{eff} for a duration of SL (t_{SL}), and then flipped back to the z-axis for imaging. The θ-degree rotation matrix [$\mathbf{R}(\theta)$] is given by Eq. (4), where $\theta=\tan^{-1}(\omega_1/\Omega)$. Thus, we obtain the magnetization after SL as $\mathbf{M}(t_{SL})=\mathbf{R}(-\theta)e^{\mathbf{A}t_{SL}}\mathbf{R}(\theta)\mathbf{M}(0)$...(5). Note that Ω and θ are 0 and $\pi/2$, respectively, for an on-resonance SL.

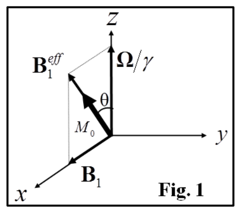

Fig. 1

$$\mathbf{R}(\theta)=\begin{pmatrix} \cos\theta & 0 & 0 & 0 & \sin\theta & 0 & 0 \\ 0 & \cos\theta & 0 & 0 & 0 & \sin\theta & 0 \\ 0 & 0 & 1 & 0 & 0 & 0 & 0 \\ 0 & 0 & 0 & 1 & 0 & 0 & 0 \\ -\sin\theta & 0 & 0 & 0 & \cos\theta & 0 & 0 \\ 0 & -\sin\theta & 0 & 0 & 0 & \cos\theta & 0 \\ 0 & 0 & 0 & 0 & 0 & 0 & 1 \end{pmatrix}\cdots(4)$$

To calculate the longitudinal relaxation time in the rotating frame ($T_{1\rho}$), the z component of magnetization in pool a for t_{SL} [$M_z^a(t_{SL})$] was fitted to the following equation: $M_z^a(t_{SL})=(M_0^a-M_{zss}^a)\exp(-t_{SL}/T_{1\rho})+M_{zss}^a$...(6), where M_{zss}^a denotes the steady-state z component of magnetization in pool a. On the other hand, Trott and Palmer [4] derived the approximate solution for $R_{1\rho}$ ($=1/T_{1\rho}$) by replacing R_1^a and R_1^b by $R_1=P_aR_1^a+P_bR_1^b$ and R_2^a and R_2^b by $R_2=P_aR_2^a+P_bR_2^b$, where P_a and P_b are the fractional sizes of pool a and pool b, and are given by $P_a=M_0^a/(M_0^a+M_0^b)$ and $P_b=M_0^b/(M_0^a+M_0^b)$, respectively: $R_{1\rho}=R_1\cos^2\theta+(R_2+R_{ex})\sin^2\theta$...(7). To validate our method, we compared the $T_{1\rho}$ or $R_{1\rho}$ values obtained by our method with or without use of the population-averaged R_1 and R_2 values with those calculated from Eq. (7). In this study, unless specifically stated, Ω=2000 Hz for an off-resonance SL, $\omega_a-\omega_b$=2400 Hz, ω_1=1000 Hz, R_1=1.5 s^{-1}, R_2=11 s^{-1}, k_{ex} ($=k_a+k_b$) =1500 s^{-1}, $k_aM_0^a=k_bM_0^b$, M_0^a=1, M_0^b=0.03, T_1^a=3 s, and T_2^a=50 ms were assumed.

RESULTS AND DISCUSSION

Figures 2, 3, and 4 show the $T_{1\rho}$ and $R_{1\rho}$ values as a function of k_{ex} ($=k_a+k_b$), ω_1, and offset frequency, respectively. (a) and (b) in Figs. 2 and 3 show the on- and off-resonance cases, respectively. The solid, dotted, and dashed curves in Figs. 2-4 show cases when the $T_{1\rho}$ and $R_{1\rho}$ values were obtained by use of Eq. (7), our method with use of the population-averaged R_1 and R_2 values, and our method without use of them, respectively. When the population-averaged R_1 and R_2 values were used, the $T_{1\rho}$ or $R_{1\rho}$ values obtained by our method (dotted curves) agreed with the approximate solutions (solid curves) given by Trott and Palmer [4] except for the case when an RF pulse with small ω_1 was applied under the on-resonance SL [Fig. 3(a)]. These results appear to indicate the validity of our method. On the other hand, when the population-averaged R_1 and R_2 values were not used, some differences were observed between them (dashed and solid curves in Figs. 2-4).

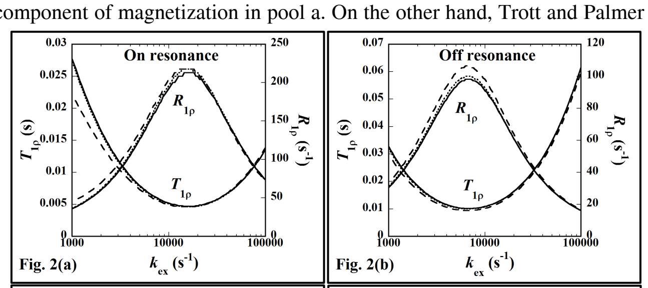

Fig. 2(a) Fig. 2(b)

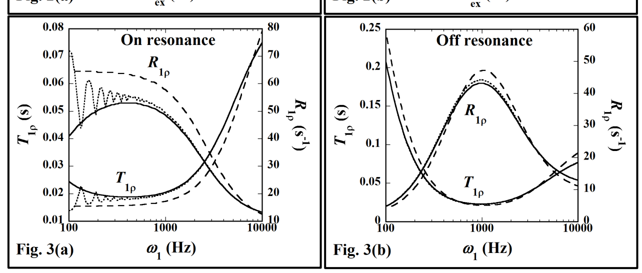

Fig. 3(a) Fig. 3(b)

As previously described, matrix operation was used in our method for solving the Bloch equations in CESTrho MRI. Although an ordinary differential equation (ODE) solver can also be used, the computation time was considerably reduced when using our method (by a factor of approximately 5000 compared to the ODE solver). In this study, we treated the 2-pool CEST model as an illustrative example. However, CEST agents often have more than one type of exchangeable proton. For such cases, it is necessary to expand the Bloch equations to multi-pool exchange models. Our method can easily be extended to multi-pool models by modifying the matrix **A** given by Eq. (2).

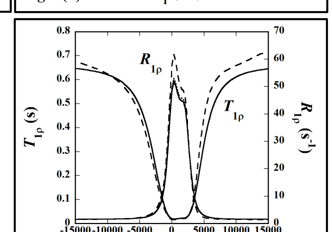

Fig. 4

CONCLUSION

We presented a simple and fast method for solving the time-dependent Bloch equations in CESTrho MRI and validated our method by comparing it with the approximate solution derived by Trott and Palmer [4]. We believe that our method will be useful for better understanding and optimization of CESTrho MRI.

REFERENCES

[1] Jin T, et al. Magn Reson Med 2011; 65:1448-1460.
[2] Kogan F, et al. Magn Reson Med 2011.
[3] Murase K, et. al. Magn Reson Imaging 2011; 29:126-131.
[4] Trott O, et.al. J Magn Reson 2002; 154:157-160.